Fuzzy Virtual Reference Model Sensorless Tracking Control for Linear Induction Motors

Cheng-Yao Hung, Peter Liu, *Member, IEEE,* and Kuang-Yow Lian, *Member, IEEE,*

Abstract

This paper introduces a fuzzy virtual reference model (FVRM) synthesis method for linear induction motor (LIM) speed sensorless tracking control. First, we represent the LIM as a T-S fuzzy model. Second, we estimate the immeasurable mover speed and secondary flux by a fuzzy observer. Third, to convert the speed tracking control into a stabilization problem, we define the internal desired states for state tracking via an FVRM. Finally, by solving a set of linear matrix inequalities (LMIs), we obtain the observer gains and the control gains where exponential convergence is guaranteed. The contributions of the approach in this paper are three folds: i) simplified approach – speed tracking problem converted to stabilization problem; ii) omit need of actual reference model – fuzzy virtual reference model generates internal desired states; and iii) unification of controller and observer design – control objectives are formulated into LMI problem where powerful numerical toolboxes solve controller and observer gains. Finally, experiments are carried out to verify the theoretical results and show satisfactory performance both in transient response and robustness.

Index Terms

TS fuzzy model, linear induction motors, sensorless control

I. Introduction

Linear induction motors (LIMs) have characteristics such as high initial thrust force, alleviation of gear between motor and the motion devices, reduced mechanical losses, relatively small physical size of motion devices, and low audible noise, etc [1]–[4]. Due to these advantages, the LIM is widely used in many industrial applications, e.g., transportation systems, conveyor systems, and factory material handling.

The mathematical model of an LIM is similar to the conventional rotary induction motor. However, the LIMs are more complicated since we must consider: i) end-effects, dependent on the speed of the mover, and ii) electromechanical coupling constants, which are larger than conventional rotary induction motors. The facts mentioned above motivate us to improve the control for LIMs. In conventional induction motor control systems (both for

C.-Y Hung is with the LCD TV Business Unit, Wistron Corporation, Taipei, Taiwan

P. Liu is with the Department of Electrical Engineering, Tamkang University, Tamsui, Taipei, 25137 Taiwan (e-mail: pliu@ieee.org)

K.-Y Lian is with the Department of Electrical Engineering, National Taipei University of Technology, Taipei, 10608 Taiwan (e-mail: kylian@ntut.edu.tw)

rotary and linear), speed sensors, such as an encoder or resolver, is necessary for the feedback system to achieve motion control. However, this necessity not only increases the cost, weight, and complexity of the overall system but also degrades the robustness and reliability. Take note that sensors for linear movement measurement are very expensive, often costing more than the standalone LIM. Therefore, the sensorless control problem is inevitable for LIMs. In the works [5], a nonlinear observer is used to estimate the flux for a rotary induction motor. Nevertheless, nonlinear observers are quite complex in structure. In the comparative study of sensorless approaches in [6]–[13], including rotor-flux model reference adaptive model (MRAS) (e.g., see [14]), torque-current MRAS, and adaptive nonlinear flux observer, rely on trial and error approaches to find suitable observer gains. In the studies [15], [16], robust adaptive control for induction motors have been proposed considering parametric uncertainties and external disturbance. In light of the above sensorless nonlinear-based control approaches of induction motors, a systematic and unified observer/controller design utilizing powerful computational tools to find suitable controller/observer gains would be advantageous.

Fuzzy representation of nonlinear systems is an important topic [17], [18]. Especially, nonlinear systems can be represented by Takagi-Sugeno (T-S) fuzzy rules with consequent parts as linear subsystems [20]. The nonlinear control problem is therefore decomposed to finding the corresponding local linear compensators (i.e., using parallel distribute compensation (PDC) approach [21], [22]) for each subsystem to achieve the desired objectives. The stability analysis is then carried out using Lyapunov direct method where the control problem is formulated into a set of linear matrix inequality problems (note that we do not abbreviate to LMI to avoid confusion). Corresponding observer/controller gains can be obtained by solving the linear matrix inequalities [23]–[26] using powerful computational toolboxes (e.g., Matlab's Linear Matrix Inequality Toolbox).

In this paper, we design a fuzzy observer to estimate the internal states using information of only the two-phase current. This however imposes a problem, immeasurable premise variables arise in the fuzzy rules which couple the estimation error dynamics with the tracking error dynamics. To solve this problem, the observer design forms a vanishing perturbation when the membership functions satisfy a Lipschitz-like condition. The observer gain and controller gain can then be separately designed based on a separation property. Note that the T-S fuzzy model of the LIM is exactly equivalent to the original dynamic equations in the region of interest, i.e., no error exists in fuzzy modeling. This implies the stability result is held in a large region which is better than typical methods based on approximated models. In addition, we introduce a fuzzy virtual reference model (FVRM) controller synthesis. Compared to the work [27], [28], where only the fuzzy observer gains are solved using linear matrix inequalities while controller gains still rely on trial and error method, the combined FVRM and fuzzy observers approach introduces two additional merits: i) rigorous proof carried out on the overall estimation and tracking stability of the nonlinear system and ii) independent tuning of the decay rate for each state. In addition, we ensure exponential convergence for both estimation and tracking errors. The overall contributions of the approach in this paper are three folds: i) simplified approach – speed tracking problem converted to stabilization problem; ii) omit need of actual reference model – fuzzy virtual reference model generates internal desired states; and iii) unification of controller and observer design – control objectives are formulated into LMI problem where powerful numerical toolboxes

solve controller and observer gains. To demonstrate the effectiveness of the proposed scheme, a practical voltage-fed LIM system is used as an example to achieve speed tracking. The experiment results achieve good performance even in low speeds.

The rest of the paper is organized as follows. In Sec. II, we introduce the full model of linear induction motor and T-S fuzzy model representation. In Sec. III, we present the T-S fuzzy observer and controller design. In Sec. IV, we address the FVRM design and implementation procedure along with the stability analysis. In Section V, the experiments are carried out to illustrate the performance control scheme. Finally, some conclusions are made in Sec. VI.

II. LIM Dynamical Model

The fifth-order dynamic model of the LIM in *a-b* stationary reference frame as follows [29]–[31]:

$$\begin{aligned}
\dot{i}_{pa} &= -\tfrac{\gamma}{\sigma} i_{pa} + \tfrac{\pi n_p}{\sigma \ell} v_m \lambda_{sb} + \tfrac{R_s}{\sigma L_s} \lambda_{sa} + \tfrac{L_s}{\sigma L_m} V_{pa} \\
\dot{i}_{pb} &= -\tfrac{\gamma}{\sigma} i_{pb} - \tfrac{\pi n_p}{\sigma \ell} v_m \lambda_{sa} + \tfrac{R_s}{\sigma L_s} \lambda_{sb} + \tfrac{L_s}{\sigma L_m} V_{pb} \\
\dot{\lambda}_{sa} &= \tfrac{L_m R_s}{L_s} i_{pa} - \tfrac{\pi n_p}{\ell} v_m \lambda_{sb} - \tfrac{R_s}{L_s} \lambda_{sa} \\
\dot{\lambda}_{sb} &= \tfrac{L_m R_s}{L_s} i_{pb} + \tfrac{\pi n_p}{\ell} v_m \lambda_{sa} - \tfrac{R_s}{L_s} \lambda_{sb} \\
\dot{v}_m &= \tfrac{F}{M} - \tfrac{F_l}{M} - \tfrac{D}{M} v_m
\end{aligned} \tag{1}$$

where $\gamma = \left(\frac{L_s R_p}{L_m} + \frac{L_m R_s}{L_s} \right)$, $\sigma = L_s L_p / L_m - L_m$, $F = \kappa \left(i_{pb} \lambda_{sa} - i_{pa} \lambda_{sb} \right)$, $\kappa = 3\pi n_p L_m / 2\ell L_s$, and

i_{pa} (i_{pb})	a-axis and b-axis primary current
V_{pa} (V_{pb})	a-axis and b-axis primary voltage
λ_{sa} (λ_{sb})	a-axis and b-axis secondary flux
v_m	mover speed
R_p (R_s)	primary (secondary) resistance
L_p (L_s)	primary (secondary) inductance
L_m	mutual inductance
ℓ	pole pitch
M	primary mass
D	viscous friction
n_p	number of pole pairs
F_l	load disturbance
F	electromechanical coupling force
κ	force constant

Remark 1: The fundamental difference between an RIM and an LIM is the finite length of the magnetic and electric circuit of the LIM along the direction of the traveling field. The open magnetic circuit causes an initiation of the

so-called longitudinal end-effects. In an LIM, as the primary moves, the secondary flux continuously shifts along the same moving direction. This linear shift will induce a resistance to a sudden increase in flux penetration at the leading front since only a gradual build-up of the flux density in the air-gap is permitted. In details, as the primary coil set of the LIM moves, a new field penetrates into the reaction rail in the entry area, whereas the existing field disappears at the exit area of the primary coil as shown in Fig. 1.

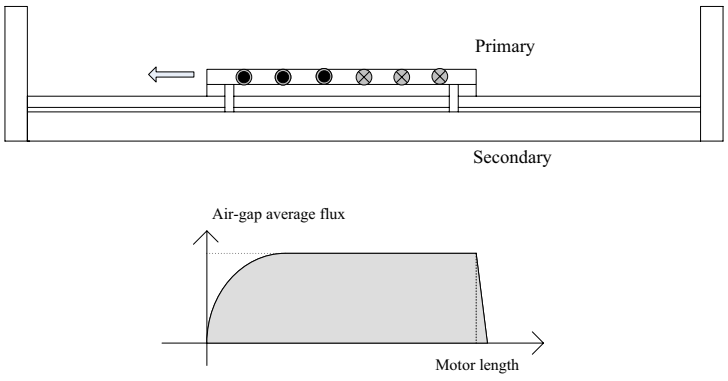

Fig. 1. Air-gap average flux distribution due to end-effect.

When the speed increases, the air-gap flux becomes more unbalanced. Since the mutual flux between the primary and the secondary is decreased by the end-effect, we can see that the equivalence of the end-effect is a reduction force as a function of speed. As we know that most functions can be described in Taylor's series, we represent the end-effect as an external force $\sum_{n=0}^{\infty} \theta_n^{'} v_m^n$, where it increases with the speed of the primary (cf. [33], [34]). As a result, for an LIM, the end-effect plus the load force can be represented as a function of the speed v_m, in the following form:

$$\begin{aligned} F_l &= \sum_{n=0}^{2} \theta_n^{'} v_m^n + F_f \\ &= \theta_0^{'} + \theta_1^{'} v_m + \theta_2^{'} v_m^2 + \theta_{f0} + \theta_{f1} v_m + \theta_{f2} v_m^2 \end{aligned} \tag{2}$$

In the following, we will truncate the series (2) with only the first three terms.

$$F_l = \theta_0 + \theta_1 v_m + \theta_2 v_m^2. \tag{3}$$

From the relationship 3, the end-effect increases with the speed of the primary. We can include the nominal part of the load force as part of the damping force, whereas the remainder effects is taken as uncertainty in the system. Conventional adaptive techniques to deal with the uncertainty lead to a complex controller design (i.e., encounter the mixed problem of simultaneously identifying the parameters and estimating state variables). Here, we propose an alternative approach to cope with this uncertainty by synthesizing a simplified robust controller where the error system is exponentially stable. ■

To represent the LIM into a T-S fuzzy model, we further rewrite Eqs. (1) as follows:

$$\begin{aligned} \dot{x}(t) &= A(x)x(t) + Bu + bF_l \\ y(t) &= Cx(t), \end{aligned} \tag{4}$$

where $x(t) = [x_1\ x_2\ x_3\ x_4\ x_5]^\top = [i_{pa}\ i_{pb}\ \lambda_{sa}\ \lambda_{sb}\ v_m]^\top$ are the overall states; $y(t) = [i_{pa}\ i_{pb}]^\top$ are the measurable outputs; $u = [V_{pa}\ V_{pb}]^\top = [u_1\ u_2]^\top$ is the control input; and the associated matrices and vector:

$$A(x) = \begin{bmatrix} -\frac{\gamma}{\sigma} & 0 & \frac{R_s}{\sigma L_s} & 0 & \frac{\pi n_p}{\sigma \ell}\lambda_{sb} \\ 0 & -\frac{\gamma}{\sigma} & 0 & \frac{R_s}{\sigma L_s} & -\frac{\pi n_p}{\sigma \ell}\lambda_{sa} \\ \frac{L_m R_s}{L_s} & 0 & -\frac{R_s}{L_s} & -\frac{\pi n_p}{\ell}v_m & 0 \\ 0 & \frac{L_m R_s}{L_s} & \frac{\pi n_p}{\ell}v_m & -\frac{R_s}{L_s} & 0 \\ -\frac{\kappa}{M}\lambda_{sb} & \frac{\kappa}{M}\lambda_{sa} & 0 & 0 & -\frac{D}{M} \end{bmatrix},$$

$$B = \begin{bmatrix} \frac{L_s}{\sigma L_m} & 0 \\ 0 & \frac{L_s}{\sigma L_m} \\ 0 & 0 \\ 0 & 0 \\ 0 & 0 \end{bmatrix}, b = \begin{bmatrix} 0 \\ 0 \\ 0 \\ 0 \\ -\frac{1}{M} \end{bmatrix}, C = \begin{bmatrix} 1 & 0 \\ 0 & 1 \\ 0 & 0 \\ 0 & 0 \\ 0 & 0 \end{bmatrix}^\top.$$

According to [27], the T-S fuzzy model rules of (4) are:

Plant Rule i :

IF λ_{sa} is F_{1i} and λ_{sb} is F_{2i} and v_m is F_{3i} THEN

$$\begin{aligned} &\dot{x}(t) = A_i x(t) + Bu(t) + bF_l \\ &y(t) = Cx(t),\ i = 1, \cdots, 8, \end{aligned} \tag{5}$$

where λ_{sa}, λ_{sb}, and v_m are immeasurable premise variables. The fuzzy sets $F_{ji} (j = 1, 2, 3)$ are set to $F_{11} = F_{12} = F_{13} = F_{14} = \frac{x_3 - d_1}{D_1 - d_1}$; $F_{15} = F_{16} = F_{17} = F_{18} = \frac{D_1 - x_3}{D_1 - d_1}$; $F_{21} = F_{22} = F_{25} = F_{26} = \frac{x_4 - d_2}{D_2 - d_2}$; $F_{23} = F_{24} = F_{27} = F_{28} = \frac{D_2 - x_4}{D_2 - d_2}$; $F_{31} = F_{33} = F_{35} = F_{37} = \frac{x_5 - d_3}{D_3 - d_3}$; and $F_{32} = F_{34} = F_{36} = F_{38} = \frac{D_3 - x_5}{D_3 - d_3}$. The system matrices A_i of subsystem i are given by

$$A_i = \begin{bmatrix} -\frac{\gamma}{\sigma} & 0 & \frac{R_s}{\sigma L_s} & 0 & \frac{\pi n_p}{\sigma \ell}\delta_i \\ 0 & -\frac{\gamma}{\sigma} & 0 & \frac{R_s}{\sigma L_s} & -\frac{\pi n_p}{\sigma \ell}\varphi_i \\ \frac{L_m R_s}{L_s} & 0 & -\frac{R_s}{L_s} & -\frac{\pi n_p}{\ell}\vartheta_i & 0 \\ 0 & \frac{L_m R_s}{L_s} & \frac{\pi n_p}{\ell}\vartheta_i & -\frac{R_s}{L_s} & 0 \\ -\frac{\kappa}{M}\delta_i & \frac{\kappa}{M}\varphi_i & 0 & 0 & -\frac{D}{M} \end{bmatrix},$$

where $\varphi_1 = D_1$, $\delta_1 = D_2$, $\vartheta_1 = D_3$; $\varphi_2 = D_1$, $\delta_2 = D_2$, $\vartheta_2 = d_3$; $\varphi_3 = D_1$, $\delta_3 = d_2$, $\vartheta_3 = D_3$; $\varphi_4 = D_1$, $\delta_4 = d_2$, $\vartheta_4 = d_3$; $\varphi_5 = d_1$, $\delta_5 = D_2$, $\vartheta_5 = D_3$; $\varphi_6 = d_1$, $\delta_6 = D_2$, $\vartheta_6 = d_3$; and $\varphi_7 = d_1$, $\delta_7 = d_2$, $\vartheta_7 = D_3$; $\varphi_8 = d_1$, $\delta_8 = d_2$, $\vartheta_8 = d_3$. In these fuzzy rules, d_1 and D_1 are accordingly the lower bound and upper bound of λ_{sa}; d_2 and D_2 are accordingly the lower bound and upper bound of λ_{sb}; d_3 and D_3 are accordingly the

upper bound and lower bound of v_m. Using the singleton fuzzifier, product fuzzy inference and weighted average defuzzifier, the inferred output of the fuzzy system

$$\begin{aligned} \dot{x}(t) &= \sum_{i=1}^{8} \mu_i(x(t)) \{A_i x(t) + Bu(t) + bF_l\} \\ y(t) &= Cx(t), \end{aligned} \tag{6}$$

where $\mu_i(x(t)) = \chi_i(x(t)) / \sum_{i=1}^{8} \chi_i(x(t))$ with $\chi_i(x(t)) = \prod_{j=1}^{3} F_{ji}(x(t))$. Note that $\sum_{i=1}^{8} \mu_i(x(t)) = 1$ for all t, where $\mu_i(x(t)) \geq 0$ for all $i = 1, \cdots, 8$. Based on F_{ji} and A_i, we can verify that the inferred output is exactly equivalent to the model of the LIM (4) in the region of interest.

Notice that the membership functions $F_{ij}(\cdot)$ satisfy $F_{ij}(x(t)) - F_{ij}(\widehat{x}(t)) = \eta_{ij}^{\top}(x(t) - \widehat{x}(t))$ for some bounded function vector $\eta_{ij}^{\top}$ and any x, $\hat{x}$ in the region of interest. We therefore conclude the following property which leads to separate observer and controller design:

Property 1: The grade function error is proportional to the estimation error $e = x - \hat{x}$, i.e.,

$$\begin{aligned} \mu_i(x(t)) - \mu_i(\widehat{x}(t)) &= \eta_{1i}^{\top}(x - \widehat{x}) F_{2i}(x) F_{3i}(x) + F_{1i}(\widehat{x}) \eta_{2i}^{\top}(x - \widehat{x}) F_{3i}(x) + F_{1i}(\widehat{x}) F_{2i}(\widehat{x}) \eta_{3i}^{\top}(x - \widehat{x}) \\ &= \Lambda_i^{\top}(x(t) - \widehat{x}(t)) \\ &= \Lambda_i^{\top} e, \end{aligned}$$

for some bounded function vector $\Lambda_i^{\top}$.

III. T-S Fuzzy Model Design of LIM

Since the mover speed and secondary flux are immeasurable, we need to design a fuzzy observer to estimate the internal states. As mentioned, the immeasurable premise variables of fuzzy rules couple the estimation error dynamics and tracking error dynamics. This leads to failure in separate design of observer gains and control gains. In addition, there exist residual estimation errors and tracking errors. Fortunately, the observer-based control design yields a vanishing perturbation if the membership functions satisfy a Lipschitz-like condition (see Property 1) which allows separately designing the observer gain and control gain.

A. Fuzzy Observer Design

We now design the fuzzy observer to estimate the immeasurable states. According to the fuzzy model (5), and assuming the pair (A_i, C) is observable, the observer rules are as follows:

Observer Rule i :

IF $\hat{\lambda}_{sa}$ is F_{1i} and $\hat{\lambda}_{sb}$ is F_{2i} and $\hat{v}_m$ is F_{3i} THEN

$$\dot{\hat{x}}(t) = A_i \hat{x}(t) + Bu(t) + bF_l + L_i(y(t) - \hat{y}(t))$$

$$\hat{y}(t) = C\hat{x}(t), \ i = 1, \cdots, 8$$

where the premise variables $\hat{\lambda}_{sa}$, $\hat{\lambda}_{sb}$, and $\hat{v}_m$ are accordingly the estimations of λ_{sa}, λ_{sb}, and v_m; $\hat{x}(t)$ and $\hat{y}(t)$ are accordingly the estimation of $x(t)$ and $y(t)$; and L_i is an observer gain to be determined later. The inferred output of the observer

$$\begin{aligned}\dot{\hat{x}}(t) &= \sum_{i=1}^{8}\mu_i(\widehat{x}(t))\{A_i\hat{x}(t)+Bu(t)+bF_l+L_i(y(t)-\hat{y}(t))\}\\ \hat{y}(t) &= C\hat{x}(t).\end{aligned} \tag{7}$$

Define the state estimation error $e(t)=x(t)-\hat{x}(t)$. Subtracting (6) by (7), we have

$$\begin{aligned}\dot{e}(t) &= \sum_{i=1}^{8}\mu_i(x(t))\{A_ix(t)+Bu(t)\}-\sum_{i=1}^{8}\mu_i(\widehat{x}(t))\{A_i\hat{x}(t)+Bu(t)+L_i(y(t)-\hat{y}(t))\}\\ &= \sum_{i=1}^{8}\mu_i(x(t))\{(A_i-L_iC)e\}+h_1(t),\end{aligned} \tag{8}$$

where $h_1(t)=\sum_{i=1}^{8}(\mu_i(x)-\mu_i(\widehat{x}))\{A_i\hat{x}+L_iCe\}$. The term $h_1(t)$ in (8) is unknown due to immeasurable premise variables λ_{sa}, λ_{sb}, and v_m.

B. Observer-based Controller Design

According to the T-S fuzzy model (5), we introduce FVRM and denote $x_d=[x_{1d}\ x_{2d}\ x_{3d}\ x_{4d}\ x_{5d}]^\intercal$which is tracked by state variable x. The control objective is for system output x_5 to track the desired output x_{5d}. Define the tracking error $\tilde{x}(t)=x(t)-x_d(t)$. The time derivative of tracking error

$$\begin{aligned}\dot{\tilde{x}}(t) &= \dot{x}(t)-\dot{x}_d(t)\\ &= \sum_{i=1}^{8}\mu_i(x(t))\{A_ix+Bu+bF_l\}-\dot{x}_d\\ &= \sum_{i=1}^{8}\mu_i(x(t))\{A_ix+Bu+bF_l\}-\dot{x}_d+\left(\overline{A}(\widehat{x})x_d+\Omega\right)-\sum_{i=1}^{8}\mu_i(\hat{x}(t))A_ix_d\\ &= \sum_{i=1}^{8}\mu_i(x(t))A_i\tilde{x}(t)+B\tau(t)+\bar{h}_2(t)\end{aligned} \tag{9}$$

where

$$B\tau(t)=Bu(t)+bF_l+\overline{A}(\widehat{x})x_d(t)-\dot{x}_d(t), \tag{10}$$

and $\bar{h}_2(t)=\sum_{i=1}^{8}(\mu_i(x(t))-\mu_i(\widehat{x}(t)))A_ix_d(t)+\Omega$. Note that the new control variable $\tau(t)$ is to be designed later and Eq. (10) will be used for applying FVRM synthesis in the upcoming section. Define

$$\overline{A}(\widehat{x})=\begin{bmatrix}-\frac{\gamma}{\sigma} & 0 & \frac{R_s}{\sigma L_s} & 0 & \frac{\pi n_p}{\sigma\ell}\hat{\lambda}_{sb}\\ 0 & -\frac{\gamma}{\sigma} & 0 & \frac{R_s}{\sigma L_s} & -\frac{\pi n_p}{\sigma\ell}\hat{\lambda}_{sa}\\ \frac{L_mR_s}{L_s} & 0 & -\frac{R_s}{L_s} & -\frac{\pi n_p}{\ell}\hat{v}_m & 0\\ 0 & \frac{L_mR_s}{L_s} & \frac{\pi n_p}{\ell}\hat{v}_m & -\frac{R_s}{L_s} & 0\\ -\frac{\kappa}{M}x_{4d} & \frac{\kappa}{M}x_{3d} & 0 & 0 & -\frac{D}{M}\end{bmatrix},$$

and $\Omega = [0\ 0\ 0\ 0\ \frac{\kappa}{M}\left(x_{1d}\left(e_4 - \tilde{x}_4\right) + x_{2d}(\tilde{x}_3 - e_3)\right)]^\top$ with $\tilde{x}_3 = x_3 - x_{3d}$, $\tilde{x}_4 = x_4 - x_{4d}$, $e_3 = x_3 - \hat{x}_3$, $e_4 = x_4 - \hat{x}_4$.

From the viewpoint of tracking error system (9), the design for $\tau(t)$ is similar to solving a stabilization problem. In other words, the control objective is for $\tilde{x}(t)$ to be zero whereas the new fuzzy controller $\tau(t)$, according to PDC, is as follows:

$$\begin{aligned}\textbf{Control Rule } i: \quad & \text{IF } \hat{\lambda}_{sa} \text{ is } F_{1i} \text{ and } \hat{\lambda}_{sb} \text{ is } F_{2i} \\ & \text{and } \hat{v}_m \text{ is } F_{3i} \text{ THEN} \\ & \tau(t) = -K_i\left\{\widehat{x}(t) - x_d(t)\right\},\end{aligned}$$

where K_i represent feedback gains. The inferred output $\tau(t) = -\sum_{i=1}^{8}\mu_i\left(\widehat{x}(t)\right)K_i\left\{\widehat{x}(t) - x_d(t)\right\}$. After substituting the control input into (9), the tracking error system

$$\begin{aligned}\dot{\tilde{x}}(t) &= \sum_{i=1}^{8}\mu_i\left(x(t)\right)A_i\tilde{x}(t) + B\tau(t) + \bar{h}_2(t) \\ &= \sum_{i=1}^{8}\mu_i\left(x(t)\right)\left\{A_i\tilde{x}(t) - BK_i(\widehat{x}(t) - x_d(t))\right\} + h_2(t) \\ &= \sum_{i=1}^{8}\mu_i\left(x(t)\right)\left\{\left(A_i - BK_i\right)\widetilde{x}(t) + BK_ie(t)\right\} + h_2(t), \end{aligned} \tag{11}$$

where $h_2(t) = \sum_{i=1}^{8}\left(\mu_i\left(x(t)\right) - \mu_i\left(\widehat{x}(t)\right)\right)\left\{A_ix_d(t) + BK_i\left(\widehat{x}(t) - x_d(t)\right)\right\} + \Omega$. By combining (8) and (11), an augmented error system

$$\dot{\Psi}(t) = \sum_{i=1}^{8}\mu_i\left(x(t)\right)\tilde{A}_i\Psi(t) + h(t), \tag{12}$$

where

$$\begin{aligned}\Psi(t) &= \begin{bmatrix} e(t) \\ \tilde{x}(t)\end{bmatrix}, \tilde{A}_i = \begin{bmatrix} A_i - L_iC & 0 \\ BK_i & A_i - BK_i\end{bmatrix}, \\ h(t) &= \begin{bmatrix} h_1(t) \\ h_2(t)\end{bmatrix}\end{aligned}$$

In (12), the term $h(t)$ can be taken as disturbance in the augmented error system.

Remark 2: According to Property 1, the perturbation $h_1(t)$ is bounded by the relationship

$$h_1^\top h_1 \le e^\top\Theta^\top\Theta e$$

with a symmetric positive-definite matrix Θ. ■

Remark 3: Suppose that $x_d(t)$ is bounded and Property 1 satisfied, the disturbance $h_2(t)$ is therefore bounded by the relationship

$$h_2^\top h_2 \le e^\top\Upsilon^\top\Upsilon e + \tilde{x}^\top\Phi^\top\Phi\tilde{x}$$

with symmetric positive-definite matrices Υ and Φ. ■

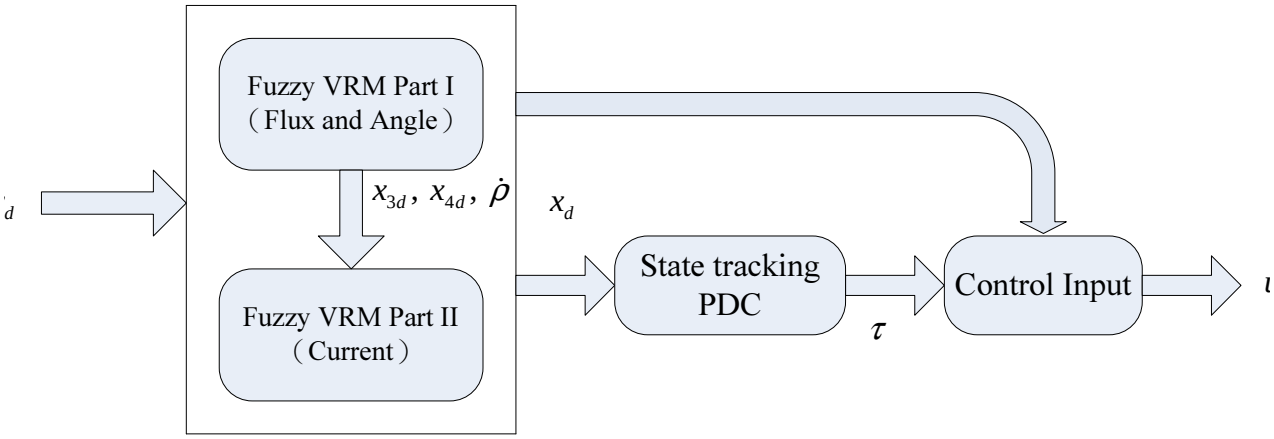

Fig. 2. The fuzzy VRM design procedure.

IV. Fuzzy VRM Implementation

In this section, we further synthesize the VRMs−the virtual desired current $(x_{1d},\ x_{2d})$ and virtual desired flux $(x_{3d},\ x_{4d})$. First, we specify the constant desired flux

$$c^2 = x_{3d}^2 + x_{4d}^2 \tag{13}$$

for the generation of an optimal force. Considering the constraint (10), we have the following expression:

$$\frac{L_s}{\sigma L_m}(\tau_1 - u_1) = -\frac{\gamma}{\sigma}x_{1d} + \frac{R_s}{\sigma L_s}x_{3d} + \frac{\pi n_p}{\sigma \ell}\hat{\lambda}_{sb}x_{5d} - \dot{x}_{1d} \tag{14}$$

$$\frac{L_s}{\sigma L_m}(\tau_2 - u_2) = -\frac{\gamma}{\sigma}x_{2d} - \frac{\pi n_p}{\sigma \ell}\hat{\lambda}_{sa}x_{5d} + \frac{R_s}{\sigma L_s}x_{4d} - \dot{x}_{2d} \tag{15}$$

$$0 = \frac{L_m R_s}{L_s}x_{1d} - \frac{R_s}{L_s}x_{3d} - \frac{\pi n_p}{\ell}\hat{v}_m x_{4d} - \dot{x}_{3d} \tag{16}$$

$$0 = \frac{L_m R_s}{L_s}x_{2d} + \frac{\pi n_p}{\ell}\hat{v}_m x_{3d} - \frac{R_s}{L_s}x_{4d} - \dot{x}_{4d} \tag{17}$$

$$0 = \frac{\kappa}{M}x_{2d}x_{3d} - \frac{\kappa}{M}x_{1d}x_{4d} - \frac{D}{M}x_{5d} - \frac{F_l}{M} - \dot{x}_{5d}. \tag{18}$$

The Eqs. (16) and (17) can be rewritten as

$$\begin{bmatrix} \dot{x}_{3d} \\ \dot{x}_{4d} \end{bmatrix} = \left(\frac{\pi n_p}{\ell}\hat{v}_m \mathbf{J}_2 - \frac{R_s}{L_s}\mathbf{I}_2\right)\begin{bmatrix} x_{3d} \\ x_{4d} \end{bmatrix} + \frac{L_m R_s}{L_s}\begin{bmatrix} x_{1d} \\ x_{2d} \end{bmatrix}, \tag{19}$$

where

$$\mathbf{I}_2 = \begin{bmatrix} 1 & 0 \\ 0 & 1 \end{bmatrix}, \mathbf{J}_2 = \begin{bmatrix} 0 & -1 \\ 1 & 0 \end{bmatrix}.$$

For simplification (along with (13)), we set

$$\begin{bmatrix} x_{3d} \\ x_{4d} \end{bmatrix} = \begin{bmatrix} c\cos(\rho(t)) \\ c\sin(\rho(t)) \end{bmatrix}, \tag{20}$$

where the variable $\rho(t)$ is determined later. We therefore have

$$\begin{bmatrix} \dot{x}_{3d} \\ \dot{x}_{4d} \end{bmatrix} = \begin{bmatrix} -\dot{\rho} x_{4d} \\ \dot{\rho} x_{3d} \end{bmatrix} = \dot{\rho} \mathbf{J}_2 \begin{bmatrix} x_{3d} \\ x_{4d} \end{bmatrix}. \tag{21}$$

Substituting (21) into (19), the desired state vector

$$\begin{bmatrix} x_{1d} \\ x_{2d} \end{bmatrix} = \left\{ \frac{L_s}{L_m R_s} \left(\dot{\rho} - \frac{\pi n_p}{\ell} \hat{v}_m \right) \mathbf{J}_2 + \frac{1}{L_m} \mathbf{I}_2 \right\} \begin{bmatrix} x_{3d} \\ x_{4d} \end{bmatrix}. \tag{22}$$

The time derivatives

$$\begin{bmatrix} \dot{x}_{1d} \\ \dot{x}_{2d} \end{bmatrix} = \frac{L_s}{L_m R_s} \left(\frac{D L_m R_s}{\kappa L_s c^2} \dot{x}_{5d} + \frac{M L_m R_s}{\kappa L_s c^2} \ddot{x}_{5d} \right) \mathbf{J}_2 \begin{bmatrix} x_{3d} \\ x_{4d} \end{bmatrix} + \left\{ \frac{L_s}{L_m R_s} \left(\dot{\rho} - \frac{\pi n_p}{\ell} \hat{v}_m \right) \mathbf{J}_2 + \frac{1}{L_m} \mathbf{I}_2 \right\} \begin{bmatrix} \dot{x}_{3d} \\ \dot{x}_{4d} \end{bmatrix}. \tag{23}$$

From (18), the time derivative

$$\dot{\rho}(t) = \frac{\pi n_p}{\ell} \hat{v}_m + \frac{D L_m R_s}{\kappa L_s c^2} x_{5d} + \frac{M L_m R_s}{\kappa L_s c^2} \dot{x}_{5d} + \frac{L_m R_s F_l}{\kappa L_s c^2}. \tag{24}$$

Finally, from (14) and (15), the control law

$$\begin{bmatrix} u_1 \\ u_2 \end{bmatrix} = \frac{\sigma L_m}{L_s} \begin{bmatrix} \dot{x}_{1d} \\ \dot{x}_{2d} \end{bmatrix} + \frac{\gamma L_m}{L_s} \begin{bmatrix} x_{1d} \\ x_{2d} \end{bmatrix} - \frac{L_m R_s}{L_s^2} \begin{bmatrix} x_{3d} \\ x_{4d} \end{bmatrix} + \frac{\pi n_p L_m}{\ell L_s} x_{5d} \begin{bmatrix} -\hat{\lambda}_{sb} \\ \hat{\lambda}_{sa} \end{bmatrix} + \begin{bmatrix} \tau_1 \\ \tau_2 \end{bmatrix}. \tag{25}$$

We illustrate the FVRM design procedure in Fig. 2. Now, we discuss the boundedness of the states of the FVRM.

Remark 4: From (20), the states of the FVRM x_{3d} and x_{4d} are always with upper bound c. By substituting (24)

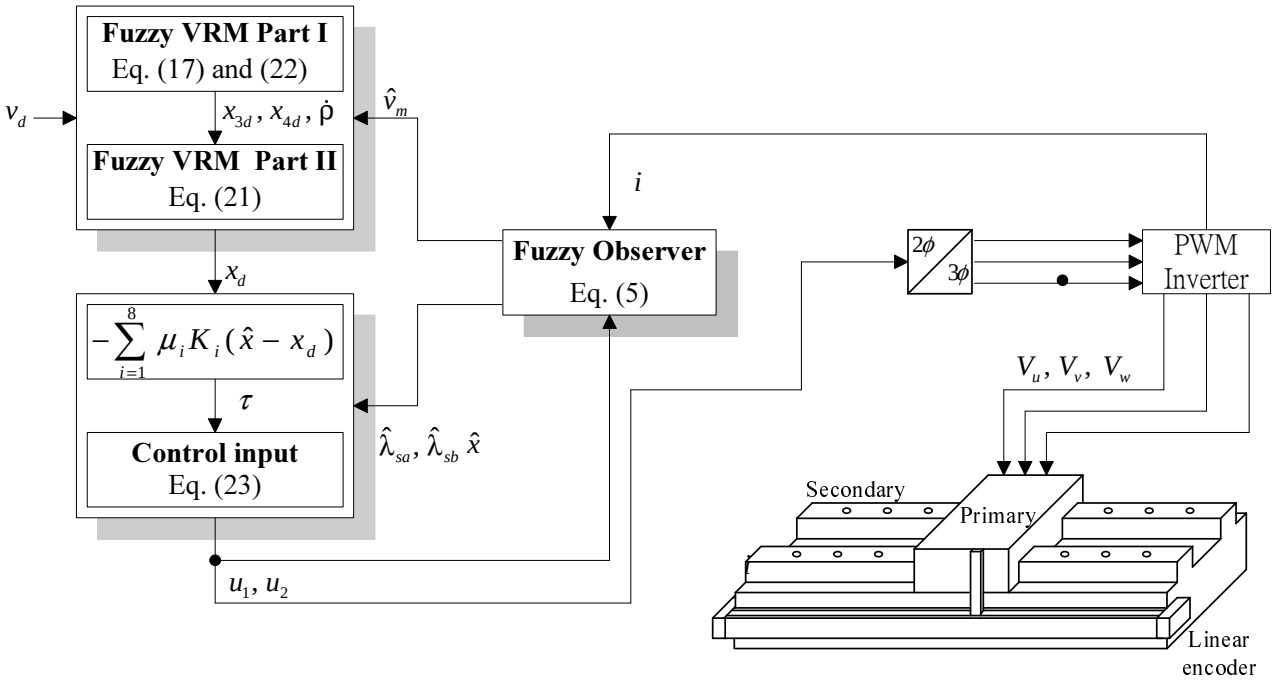

Fig. 3. The overall structure of the T-S fuzzy model-based VRM control.

into (22), we can find x_{1d} and x_{2d} depend only on x_{3d}, x_{4d}, and x_{5d}. In turn, we have x_{1d}, $x_{2d} \in L_\infty$. All of the states of the FVRM are therefore always bounded. In addition, from (24), if the estimation $\hat{v}_m$ is bounded, then the terms $\dot{\rho}$, $\dot{x}_{3d}$, and $\dot{x}_{4d}$ are bounded. In addition, from (23), the variables $\dot{x}_{1d}$ and $\dot{x}_{2d}$ are bounded when $\hat{v}_m$ is bounded. As a result, the control inputs u_1 and u_2 are bounded once $\hat{x}$ belongs to L_∞. Therefore, the stability of the overall error dynamics (12) can be carried out in the next subsection. ■

Remark 5: Here, note that u_1 and u_2 are somewhat complicated to compute due to the terms of $\dot{x}_{1d}$ and $\dot{x}_{2d}$. To simplify the implementation of u_1 and u_2, we use the approximation of $\dot{x}_{1d}$ and $\dot{x}_{2d}$. We use the fact that differentiation of a signal can be approximated and realized by a high pass filter. Here, the relationship $\dot{\bar{x}}_{1d} + \bar{x}_{1d} = x_{1d}$ in Laplace domain is $\bar{x}_{1d} = (\frac{1}{s+1})x_{1d}$ which means the variable $\bar{x}_{1d}$ denotes the low pass signal of x_{1d}. Therefore, the original signal x_{1d} subtracted by the low pass filtered signal $\bar{x}_{1d}$ results in the high pass filtered signal which leads to $\dot{x}_{1d} \approx x_{1d} - \bar{x}_{1d}$. This is also true for $\dot{x}_{2d}$. From experimental results shown later, only slight difference in transient response exist between using the complete practical control inputs and the approximate ones. In order to make the experimental result consistent with the theoretical derivations, we use complete practical control inputs (25) in our experiments. ■

The overall structure of the T-S fuzzy observer and FVRM controller is illustrated in Fig. 3.

A. Stability Analysis

Now, we discuss the stability of the overall control system. Consider the Lyapunov function candidate $V(\Psi(t)) = \Psi^\top(t) P \Psi(t)$ with P is chosen in the following form: $P = diag\{P_1, \phi P_2\}$, where P_1 and P_2 are symmetric positive-definite matrices and $\phi > 0$. The time derivative

$$\begin{aligned} \dot{V}(\Psi(t)) &= \dot{\Psi}^\top(t) P \Psi(t) + \Psi^\top(t) P \dot{\Psi}(t) \\ &= \sum_{i=1}^{8} \mu_i(x(t)) \Psi^\top(t) \left(\tilde{A}_i^\top P + P \tilde{A}_i \right) \Psi(t) + h^\top P \Psi + \Psi^\top P h. \end{aligned}$$

Note that

$$\begin{aligned} h^\top P \Psi + \Psi^\top P h &\leq h_1^\top h_1 + e^\top P_1 P_1 e + \phi \left(h_2^\top h_2 + \tilde{x}^\top P_2 P_2 \tilde{x} \right) \\ &\leq e^\top \Theta^\top \Theta e + e^\top P_1 P_1 e + \phi \left(e^\top \Upsilon^\top \Upsilon e + \tilde{x}^\top \Phi^\top \Phi \tilde{x} + \tilde{x}^\top P_2 P_2 \tilde{x} \right), \end{aligned}$$

where we use the definition of $h(t)$; and apply Remarks 1, 2 (which is held by Remark 3). Hence, further derivations lead to

$$\begin{aligned} \dot{V}(\Psi(t)) &\leq \sum_{i=1}^{8} \mu_i(x(t)) \Psi^\top \begin{bmatrix} H_i + \phi \Upsilon^\top \Upsilon & \phi K_i^\top B^\top P_2 \\ \phi P_2 B K_i & \phi G_i \end{bmatrix} \Psi - \Psi^\top \begin{bmatrix} R_1 P_1 R_1 & 0 \\ 0 & \phi (R_2 P_2 R_2) \end{bmatrix} \Psi \\ &\leq \sum_{i=1}^{8} \mu_i(x(t)) \Psi^\top \begin{bmatrix} H_i & \phi K_i^\top B^\top P_2 & \sqrt{\phi} \Upsilon^\top \\ \phi P_2 B K_i & \phi G_i & 0 \\ \sqrt{\phi} \Upsilon & 0 & -I \end{bmatrix} \Psi - \Psi^\top \begin{bmatrix} R_1 P_1 R_1 & 0 \\ 0 & \phi (R_2 P_2 R_2) \end{bmatrix} \end{aligned} \quad (26)$$

where $H_i = A_i^\top P_1 + P_1 A_i - C^\top L_i^\top P_1 - P_1 L_i C + \Theta^\top \Theta + P_1 P_1 + R_1 P_1 R_1$ and $G_i = A_i^\top P_2 + P_2 A_i - K_i^\top B^\top P_2 - P_2 B K_i + \Phi^\top \Phi + P_2 P_2 + R_2 P_2 R_2$ with R_1 and R_2 as prescribed decay rates of observer and tracking errors,

respectively. Therefore, we separately design the observer gains L_i and control gains K_i according to the following theorem.

Theorem 1: Assume the desired speed satisfies x_{5d}, $\dot{x}_{5d}$, $\ddot{x}_{5d} \in L_\infty$. The augmented error system (12) is exponentially stable if there exist common symmetric positive-definite matrices X *and* P_1 such that the following linear matrix inequalities:

$$\text{Given } R_1,\ R_2 > 0$$

$$\begin{bmatrix} A_i^\top P_1 + P_1 A_i - C^\top N_i^\top - N_i C + \Theta^\top \Theta + R_1 P_1 R_1 & P_1 \\ P_1 & -I \end{bmatrix} < 0 \tag{27}$$

$$\begin{bmatrix} X A_i^\top + A_i X - M_i^\top B^\top - B M_i + I & X\Phi^\top & X R_2^\top \\ \Phi X & -I & 0 \\ R_2 X & 0 & -X \end{bmatrix} < 0 \tag{28}$$

are feasible for $i = 1, \cdots, 8$, where $N_i = P_1 L_i$, $M_i = K_i X$, and $X = P_2^{-1}$.

Proof: Using Schur's complement, the first matrix of Eq. (26) is negative definite if and only if the following inequalities are held $(i = 1, \cdots, 8)$:

$$H_i < 0 \tag{29}$$

$$G_i - \phi\left(P_2 B K_i\right) H_i^{-1} \left(K_i^\top B^\top P_2\right) < 0. \tag{30}$$

If the inequalities (29) and $G_i < 0$ are satisfied, there exists a small ϕ such that (30) is held. In other words, we can reduce the stability condition to solve $H_i < 0$ and $G_i < 0$. As a result, we have

$$\dot{V}\left(\Psi\right) \leq -\Psi^\top \begin{bmatrix} R_1 P_1 R_1 & 0 \\ 0 & \phi\left(R_2 P_2 R_2\right) \end{bmatrix} \Psi$$

if linear matrix inequalities (27) and (28) are feasible. Hence, the exponential stability for the augmented error system is proven. ■

The exponential stability of the augmented error system (12) ensures the exponential convergence of errors to zero. In general cases, the residue of tracking error arises due to existence of $h\left(t\right)$. Some methods (such as [35]) can be used to analyze the effect of $h\left(t\right)$. However, due to the coupling of the observer gains and the control gains, the dimensions of linear matrix inequalities are large, often leading to infeasibility. In contrast, we can separately solve (27) and (28) to get the observer gains L_i and control gains K_i from the proposed control design in this paper.

Remark 6: In solving linear matrix inequalities (27) and (28), the positive definite matrixes R_1 and R_2 are given to prescribe the decay rates of observer error and tracking error, respectively. ■

V. Experimental Results

To further verify the validity of the proposed scheme, several experiments of sensorless speed control are described in this section. The experimental setup is shown in Fig. 4. The controller is realized by a DSP-based control card

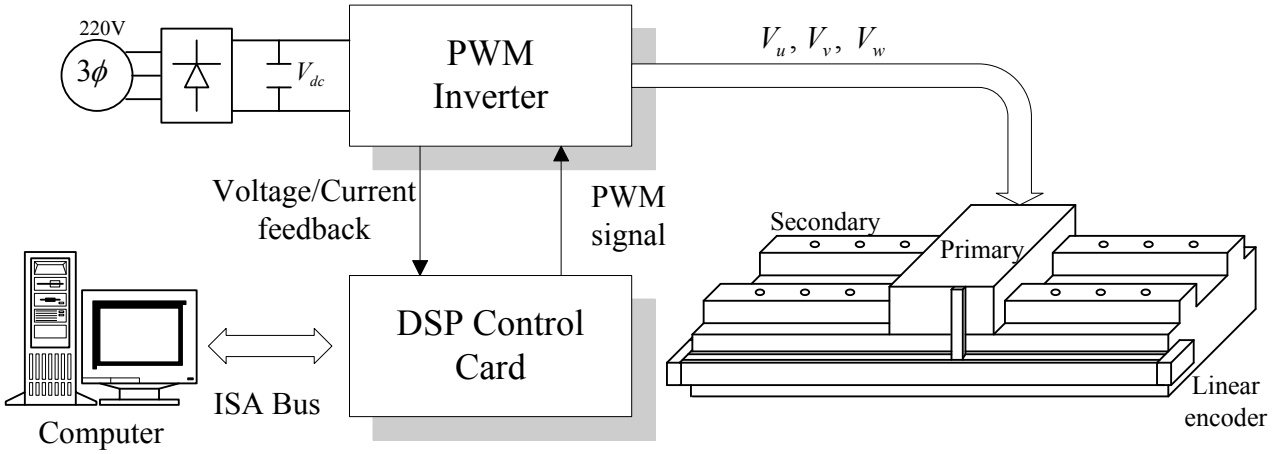

Fig. 4. The experimental setup.

TABLE I

SPECIFICATIONS AND PARAMETERS OF THE LINEAR INDUCTION MOTOR

Rated Specification	
Pole Pair	2
Power	1 HP
Voltage	240 V
Current	5 A
Pole pitch	0.0465 m
Secondary length	0.82 m
Parameters	
R_p	13.2 Ω
R_s	11.78 Ω
L_p	0.42 H
L_s	0.42 H
L_m	0.4 H
M	4.775 kg
D	53 kg/s

(Simu-Drive system), which takes the TMS320F2812 DSP (fixed-point 32-bit) as the main control core. The DSP control card also provides multichannel of A/D and encoder interface circuits. Here, three-phase voltages and currents are sampled by the A/D converters and fed into the DSP-based controller. The speed is measured by a linear encoder with precision 20μm for one pulse. In addition, the block-building MATLAB Simulink Toolbox and Real-Time Workshop are taken as an interface between software and hardware. When the build-up controller block is established, the Real-Time Workshop plays a role of a compiler to transform the controller into a C code, which is download to the DSP-based control card. The specifications and parameters of the LIM are listed in Table I.

Here, choose $c = 0.46$. Assume the immeasurable premise variables $\hat{\lambda}_{sa} \in \begin{bmatrix} D_1 & d_1 \end{bmatrix} = \begin{bmatrix} 0.8 & -0.8 \end{bmatrix}$, $\hat{\lambda}_{sb} \in \begin{bmatrix} D_2 & d_3 \end{bmatrix} = \begin{bmatrix} 0.8 & -0.8 \end{bmatrix}$, and $\hat{v}_m \in \begin{bmatrix} D_3 & d_3 \end{bmatrix} = \begin{bmatrix} 4 & -4 \end{bmatrix}$. According to LMIs (27) and (28), we let $\Phi = diag\{1.7,\ 1.5,\ 1.1,\ 0.1,\ 2.4\}$, $\Theta = diag\{0.9,\ 0.5,\ 0.5,\ 0.4,\ 2.81\}$, $R_1 = diag\{12,\ 1.9,\ 7,\ 7.3,\ 1.9\}$, and $R_2 = diag\{2.7,\ 3.9,\ 1.8,\ 1.7,\ 0.7\}$, then using the LMI toolbox of MATLAB to solve the accordingly the observer gains and control gains:

$$L_i = \begin{bmatrix} -524.9 & l_{i1} \\ l_{i2} & -599.4 \\ 217.9 & l_{i3} \\ l_{i4} & 217.9 \\ l_{i5} & l_{i6} \end{bmatrix},$$

$$K_i = \begin{bmatrix} -23.1 & k_{i1} & 27.3 & k_{i2} & k_{i3} \\ k_{i4} & -22.6 & k_{i5} & 27.1 & k_{i6} \end{bmatrix},$$

where the entries of observer gains $l_i = (l_{i1},\ l_{i2},\ l_{i3},\ l_{i4},\ l_{i5},\ l_{i6})$ are

$$\begin{aligned}
l_1 &= (-358.2,\ 358.2,\ -0.05,\ -0.002,\ 968.2,\ -968.2), \\
l_2 &= (195.9,\ -195.9,\ 0.05,\ 0.007,\ 968.2,\ -968.2), \\
l_3 &= (401.2,\ -401.2,\ -0.05,\ 0.02,\ -968.2,\ -968.2), \\
l_4 &= (735.8,\ -735.8,\ 0.04,\ -0.01,\ -968.2,\ -968.2), \\
l_5 &= (-126.7,\ 126.7,\ -0.05,\ -0.009,\ 968.2,\ 968.2), \\
l_6 &= (60.1,\ -60.1,\ 0.05,\ 0.01,\ 968.2,\ 968.2), \\
l_7 &= (494.1,\ -494.1,\ -0.05,\ -0.03,\ -968.2,\ 968.2), \\
l_8 &= (-133.8,\ 133.8,\ 0.05,\ 0.01,\ -968.2,\ 968.2);
\end{aligned}$$

and entries of control gains $k_i = (k_{i1},\ k_{i2},\ k_{i3},\ k_{i4},\ k_{i5},\ k_{i6})$ are

$$\begin{aligned}
k_1 &= (25.7,\ 0.01,\ 306.6,\ -15.3,\ -0.02,\ -307.5), \\
k_2 &= (-22.3,\ -0.02,\ 306.6,\ 13.3,\ 0.02,\ -307.5), \\
k_3 &= (-224.8,\ 0.1,\ -306.6,\ 134,\ -0.09,\ -307.5), \\
k_4 &= (-13.7,\ -0.02,\ -306.6,\ 8.2,\ 0.02,\ -307.5), \\
k_5 &= (700.9,\ -0.3,\ 306.6,\ -417.8,\ 0.1,\ 307.5), \\
k_6 &= (-193.5,\ 0.06,\ 306.6,\ 115.3,\ -0.02,\ 307.5), \\
k_7 &= (-500.1,\ 0.2,\ -306.6,\ 298.1,\ -0.1,\ 307.5), \\
k_8 &= (-554.2,\ 0.2,\ -306.6,\ 330.3,\ -0.1,\ 307.5).
\end{aligned}$$

Based on this setting, the following speed control experiments are performed.

Experiment 1: Speed Regulation

Consider speed regulation with reference $v_d = 0.5m$/sec. The desired and actual speed, actual and estimated speed are shown in Figs. 5(a) and 5(b), respectively. The speed estimation error is shown in Fig. 5(c). The primary voltage of u-phase V_u and primary current of u-phase i_u are shown in Figs. 6(a) and 6(b), respectively. Furthermore, the desired and estimated secondary flux of one phase are shown in Fig. 6(c).

Consider speed regulation with reference $v_d = 0.3m/\sec$ with an abrupt external load variation. To generate such external force in this experiment, a $1kg$ load is placed gently on the moving table during operating. The external force is added at $t = 0.7\sec$ and removed at $t = 1.4\sec$. The experimental results for the desired and actual speed is shown in Fig. 7(a) and actual and estimated speed is shown in Fig. 7(b). The speed estimation error is shown in Fig. 7(c). The primary voltage of u-phase V_u and primary current of u-phase i_u are shown in Figs. 8(a) and 8(b), respectively.

Experiment 2: Sinusoidal Speed Tracking

Consider the speed tacking for a sinusoidal reference $v_d = 0.5\sin\pi t\ m/\sec$. The desired and actual speed is shown in Fig. 9(a) and actual and estimated speed in Fig. 9(b). The speed estimation error is shown in Fig. 9(c). The primary voltage of u-phase V_u and primary current of u-phase i_u are shown in Figs. 10(a) and 10(b), respectively. Furthermore, the desired and estimation secondary flux of one phase are shown in Fig. 10(c).

In order to investigate the robustness of the proposed control scheme, the primary and secondary resistance variations are considered here, i.e., assuming the actual $\overline{R}_s$ and $\overline{R}_p$ to be $R_s * 1.2$ and $R_p * 1.4$, respectively. Then, experimental results for the desired and actual speed, actual and estimated speed, speed estimation error are shown in Figs. 11(a), 11(b), and 11(c), respectively. The primary voltage of u-phase V_u and primary current of u-phase i_u are shown in Figs. 12(a) and 12(b), respectively.

Experiment 3: Triangular Speed Tracking

Consider a triangular speed reference illustrated in Fig. 13(a). The desired and actual speed is shown in Figs. 13(a) and actual and estimated speed in Fig. 13(b). The speed estimation error is shown in Fig. 13(c). The primary voltage of u-phase V_u and primary current of u-phase i_u are shown in Figs. 14(a) and 14(b), respectively. Moreover, the error between the desired flux and the estimated flux tends to zero through time, whereas they are not shown due to space consideration.

Experiment 4: Low Speed Regulation

Consider a speed regulation with reference $v_d = 5cm/\sec$. The desired and actual speed is shown in Figs. 15(a) and actual and estimated speed in Fig. 15(b). The speed estimation error is shown in Fig. 15(c). The primary voltage of u-phase V_u and primary current of u-phase i_u are shown in Figs. 16(a) and 16(b), respectively.

From these figures, we can find that the estimation errors and the tracking errors have fast convergence rate. Furthermore, the primary current response, primary voltage, and the states of the FVRM evolve in a reasonable region. The satisfactory performance has been illustrated even in the situations of load uncertainties, parametric uncertainties and low speed control.

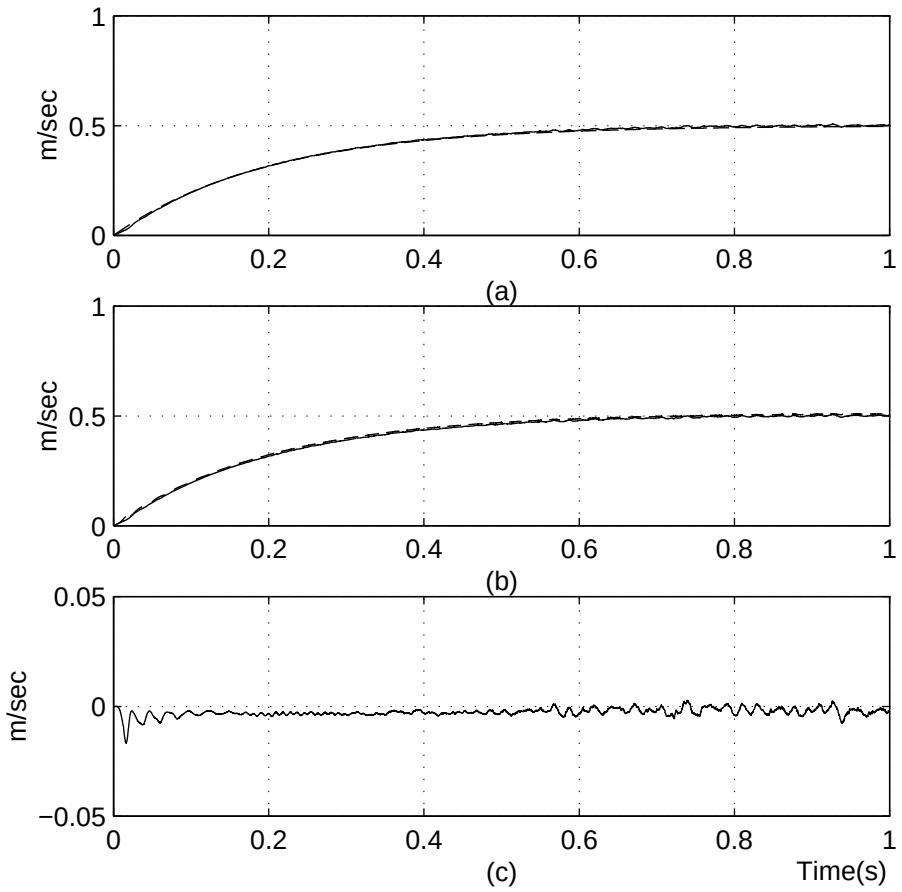

Fig. 5. Speed regulation, (a) desired speed (−−) and actual speed (—), (b) estimated speed (−−) and actual speed (—), (c) speed estimation error.

VI. CONCLUSIONS

This paper has presented a sensorless speed control scheme for LIM via the FVRM design. For sensorless speed control, we use a fuzzy observer to estimate the mover speed and secondary flux of a LIM. Besides, the fuzzy observer and the fuzzy controller are independently constructed where the overall fuzzy controller is designed via FVRM synthesis, such that the control input steers the state variables toward the virtual desired signals. Moreover, the observer gains and control gains are obtained by independently solving linear matrix inequalities. The estimated speed rapidly converges to the actual speed after the initial transient time, and the tracking errors approximate to zero. One more thing that deserves to be mentioned is that the stability discussed in this paper is exponentially stable. This means that the system under our proposed control method is very robust and tolerate uncertainty. Finally, the experimental results not only illustrate satisfactory performance, but also indicate that the proposed scheme is suitable to practical applications.

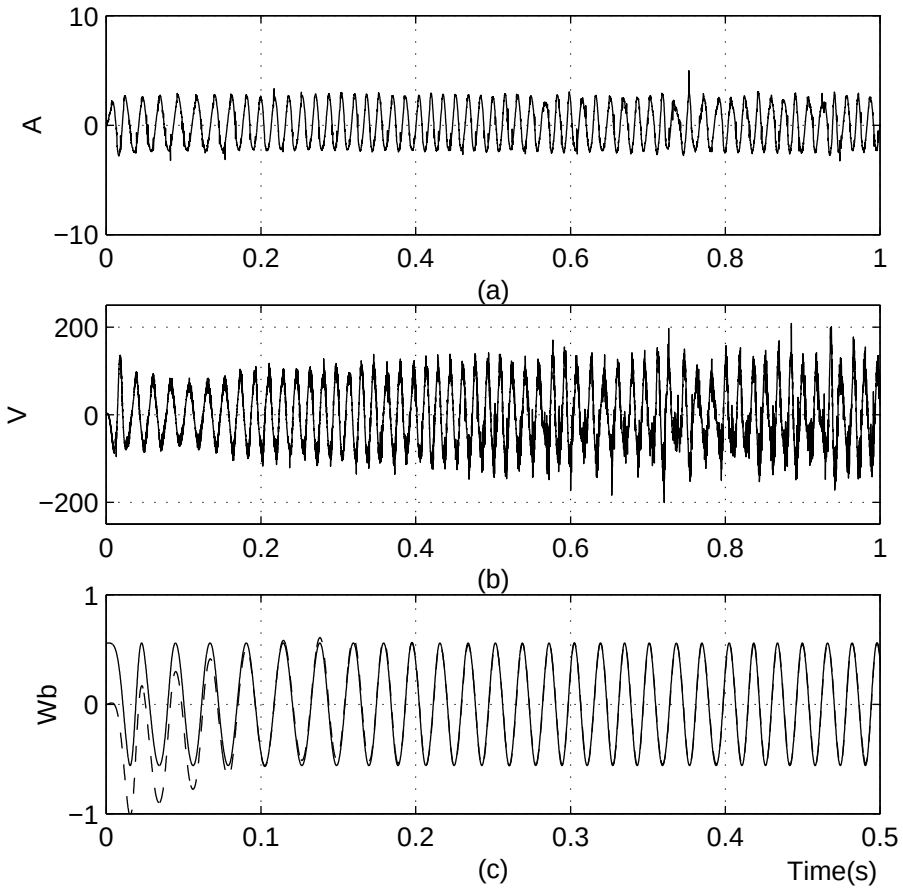

Fig. 6. Speed regulation, (a) primary current for one phase, (b) primary voltage for one phase (c) estimated (−−) and desired (—) secondary fluxes λ_{sa}.

ACKNOWLEDGMENT

This work was supported by National Science Council, R.O.C., under grant NSC 99-2221-E032-029.

REFERENCES

[1] I. Takahashi and Y. Ide, "Decoupling control of thrust and attractive force of a LIM using a space vector control inverter," *IEEE Trans. Ind. Appl.,* vol. 29, no. 1, pp. 161-167, 1993.

[2] Z. Zhang, T. R. Eastham and G. E. Dawson, "Peak thrust operation of linear induction machines from parameter identification," *IEEE Industry Applications Thirtieth IAS Annual Meeting,* Orlando, Florida USA, vol. 1, pp. 375-379, 1995.

[3] G. H. Abdou and S. A. Sherif, "Theoretical and experimental design of LIM in automated manufacturing systems," *IEEE Trans. Ind. Appl.*, vol. 27, no. 2, pp. 286-293, 1991.

[4] C. I. Huang and L. C. Fu, "Adaptive approach to motion controller of linear induction motor with friction compensation," *IEEE/ASME Trans. Mechatronics*, vol. 12, no. 4, pp. 480-490, 2007

[5] M. Rodič and K. Jezernik, "Speed-Sensorless Sliding-Mode Torque Control of an Induction Motor," *IEEE Trans. Ind. Elect.,* vol. 49, no. 1, pp. 87-95, 2002.

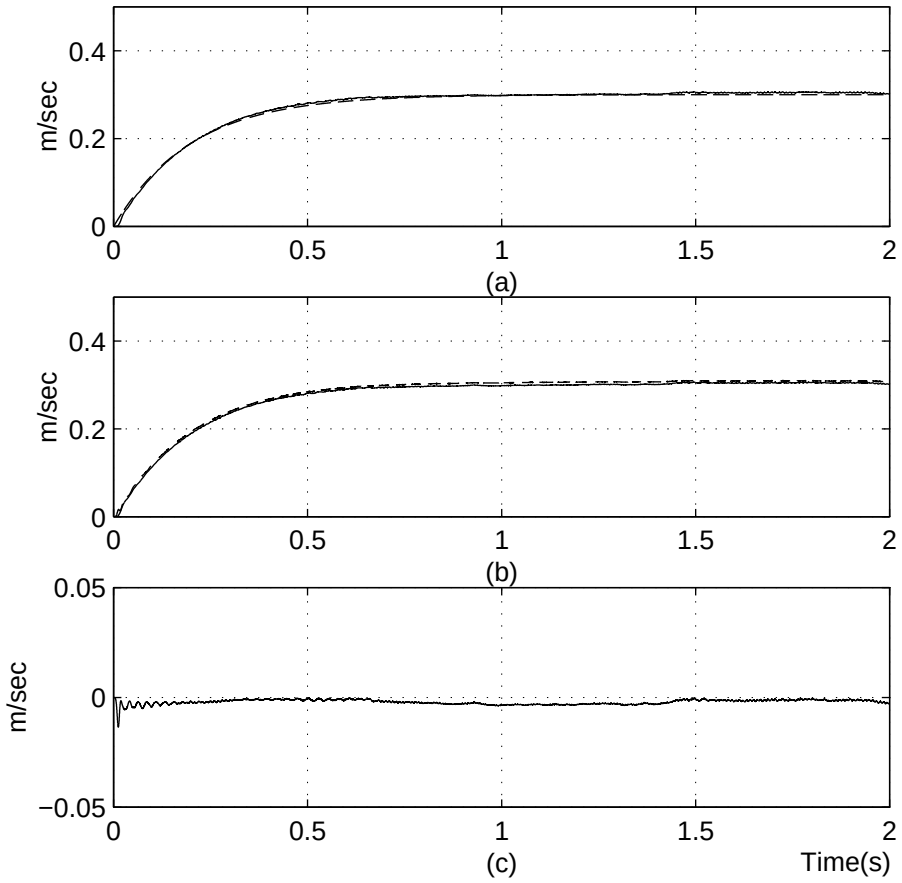

Fig. 7. Speed regulation with abrupt load variation, (a) desired speed (−−) and actual speed (—), (b) estimated speed (−−) and actual speed (—), (c) speed estimation error.

[6] K. Ohyama, G. M. Asher and M. Summer, "Comparative Analysis of Experimental Performance and Stability of Sensorless Induction Motor Drives," *IEEE Trans. Ind. Elect.*, vol. 53, no. 1, pp. 178-186, 2006.

[7] L. Mengwei, J. Chiasson, M. Bodson and L.M. Tolbert, "A differential-algebraic approach to speed estimation in an induction motor," *IEEE Trans. on Automatic Control*, vol. 51, no. 7, pp. 1172 - 1177, 2006.

[8] M. Ghanes, and Z. Gang, "On Sensorless Induction Motor Drives: Sliding-Mode Observer and Output Feedback Controller," *IEEE Trans. on Ind. Elect.*, vol. 56, no. 9, pp. 3404 -3413, 2009.

[9] M. Ghanes, J.-B. Barbot, J. De Leon, and A. Glumineau, "A robust sensorless output feedback controller of the induction motor drives: new design and experimental validation," *Int'l J. of Cont.*, vol. 83, no. 3, pp. 484-497, 2010.

[10] M.S. Zaky, "Stability Analysis of Speed and Stator Resistance Estimators for Sensorless Induction Motor Drives," *IEEE Trans. on Ind. Elect.*, vol. 59, no. 2, pp. 858 -870, 2012.

[11] G.R.A. Markadeh, E. Daryabeigi, C. Lucas, and M.A. Rahman, "Speed and Flux Control of Induction Motors Using Emotional Intelligent Controller," *IEEE Trans. on Industry App.,* vol. 47, no. 3, pp. 1126 -1135, 2011.

[12] H. Amirkhani and A. Shoulaie, "Online control of thrust and flux in linear induction motors," *IEE Proc. Electr. Power Appl.*, vol. 150, no. 5, pp. 515-520, 2003.

[13] H. M. Ryu, J. I. Ha and S. K. Sul, "A new sensorless thrust control of linear induction motor," *IEEE Industry Applications Thirty-Fifth IAS Annual Meeting*, Roma, Italy, pp. 1655-1661, 2000

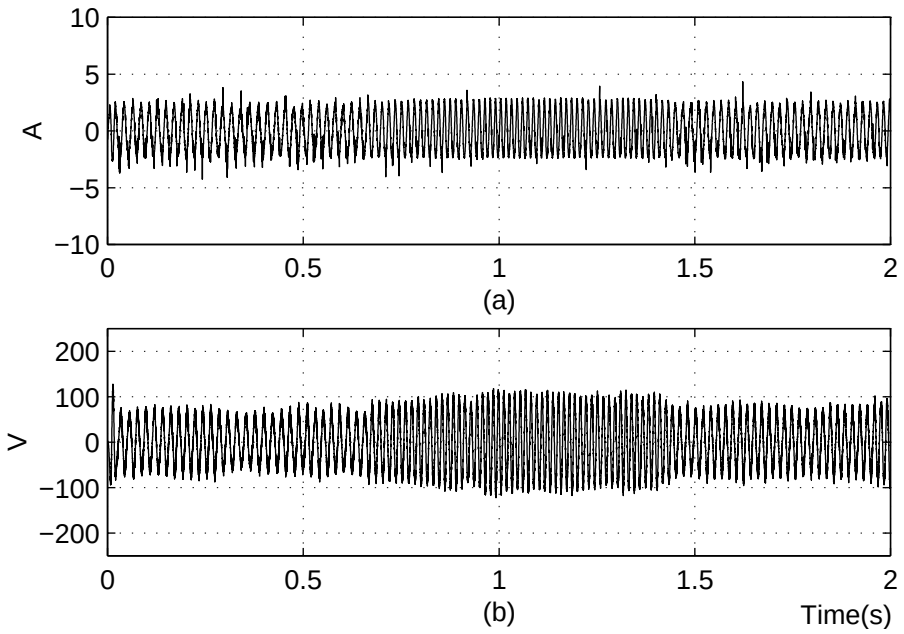

Fig. 8. Speed regulation with abrupt load variation, (a) primary current for one phase, (b) primary voltage for one phase.

[14] V. R. Jevremovic, V. Vasic, D. P. Marcetic and B. Jeftenic, "Speed-sensorless control of induction motor based on reactive power with rotor time constant identification," *IET Electr. Power Appl.*, vol. 4, no. 6, pp. 462-473, 2010.

[15] O. Barambones and A. J. Garrido, "Adaptive sensorless robust control of AC drives based on sliding mode control theory," *Int. J. Robust Nonlinear Control*, vol. 17, pp. 862–879, 2007

[16] P. Tomei, C. M. Verrelli, M. Montanari and A. Tilli, "Robust output feedback learning control for induction motor servo drives," *Int. J. Robust Nonlinear Control*, vol. 19, pp. 1745–1759, 2009.

[17] H. Zhang and Y. Quan , "Modeling, identification, and control of a class of nonlinear systems," *IEEE Trans. Fuzzy Syst.,* vol. 9, no. 2, pp. 349 -354, 2001.

[18] H. Zhang, Y. Wang and D. Liu, "Delay-Dependent Guaranteed Cost Control for Uncertain Stochastic Fuzzy Systems With Multiple Time Delays," *IEEE Trans. on Systems, Man, and Cybernetics, Part B: Cyber.,* vol. 38, no. 1, pp. 126 -140, 2008.

[19] F. Cupertino, A. Lattanzi and L. Salvatore, "A new fuzzy logic-based controller design method for DC and AC impressed-voltage drives," *IEEE Trans. Power Electronics*, vol. 15, no. 6, pp. 974-982, 2000.

[20] T. Takagi and M. Sugeno, "Fuzzy identification of systems and its applications to modeling and control," *IEEE Trans. Syst., Man, Cybern.,* vol. 15, pp. 116-132, 1985.

[21] H. O. Wang, K. Tanaka and M. F. Griffin, "An approach to fuzzy control of nonlinear systems: Stability and design issues," *IEEE Trans. Fuzzy Syst.,* vol. 4, no. 1, pp. 14-23, 1996

[22] M. Sugeno and G. T. Kang, "Fuzzy modeling and control of multilayer incinerator," *Fuzzy Sets Syst.,* vol. 60, pp. 329-346, 1986.

[23] K. Y. Lian, C. S. Chiu, T. S. Chiang and P. Liu, "LMI-based fuzzy chaotic synchronization and communications," *IEEE Trans. Fuzzy Syst.,* vol. 9, no. 4, pp. 539-553, 2001

[24] K. Tanaka and H. O. Wang, *Fuzzy Control Systems Analysis and Design: A Linear Matrix Inequality Approach*. New York: Wiley, 2000.

[25] X. J. Ma, Z. Q. Sun and Y. Y. He, "Analysis and design of fuzzy controller and fuzzy observer," *IEEE Trans. Fuzzy Syst.,* vol. 6, no. 1, pp. 41-51, 1998.

[26] M. Narimani, H. K. Lam, R. Dilmaghani and C. Wolfe, "LMI-Based Stability Analysis of Fuzzy-Model-Based Control Systems Using Approximated Polynomial Membership Functions," *IEEE Trans. on Systems, Man, and Cybernetics, Part B: Cyber.,* vol. 41, no. 3, pp.

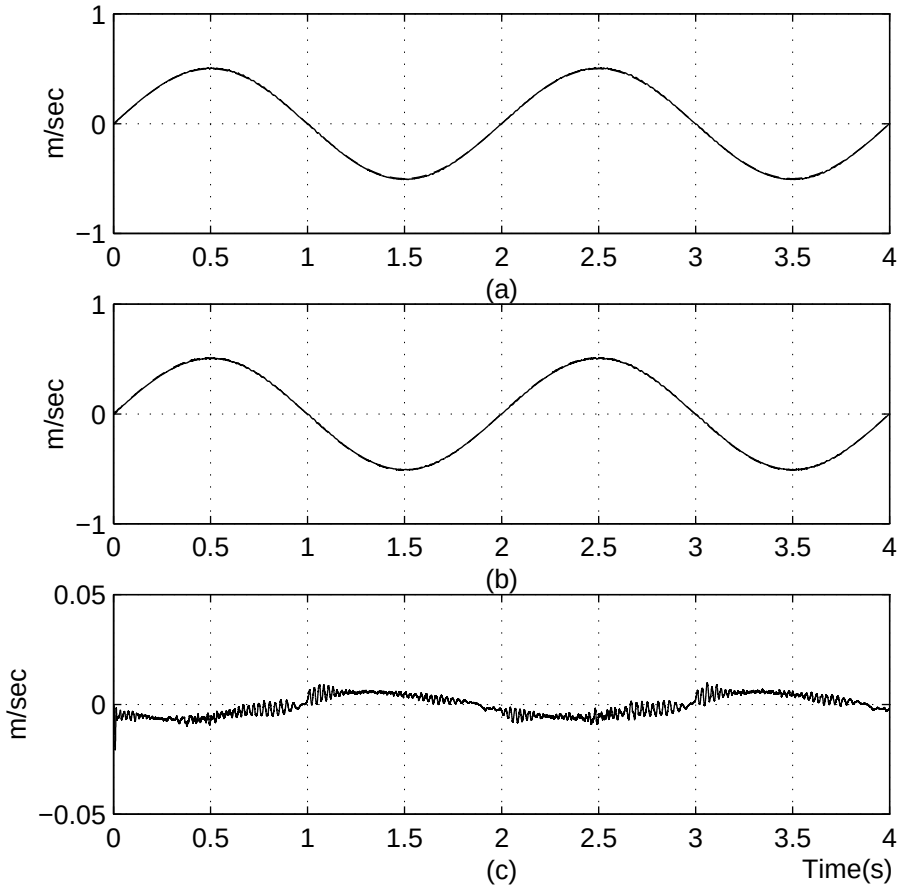

Fig. 9. Sinusoidal speed tracking, (a) desired speed (− −) and actual speed (—), (b) estimated speed (− −) and actual speed (—), (c) speed estimation error.

713-724, 2011.

[27] K. Y. Lian and C. Y. Hung, "Sensorless control for induction motors via fuzzy observer design," *in Proc. ISIE*, Montréal, Canada, pp. 2140-2145, 2006.

[28] P. Liu, C. Y. Hung, C. S. Chiu and K. Y. Lian, "Sensorless Linear Induction Motor Speed Tracking using Fuzzy Observers," to appear in *IET Electr. Power Appl.*

[29] I. Boldea and S. A. Nasar, *Linear Electric Actuators and Generators*, Cambridge, U.K.: Cambridge Univ. Press, 1997.

[30] S. A. Nasar and I. Boldea, *Linear Motion Electric Machines*. John Wiley & Sons, Inc., 1976.

[31] B. K. Bose, *Power Electronics and Motor Drives: Advances and Trends.* Academic Press, 2006.

[32] K. Y. Lian, C. Y. Hung, C. S. Chiu and P. Liu, "Induction motor control with friction compensation: An approach of virtual-desired-variable synthesis," *IEEE Trans. Power Electr.,* vol. 20, no. 5, pp. 1066-1074, 2005.

[33] E. F. Silva, C. C. Santos and J. W. L. Nerys, "Field oriented control of linear induction motor taking into account end-effects," *in Proc. AMC*, Kawasaki, Japan, March. pp. 689-694, 2004.

[34] J. H. Sung and K. Nam, "A new approach to vector control for a linear induction motor considering end effects," *IEEE Industry Applications Thirty-Fourth IAS Annual Meeting*, Phoenix, Arizona USA. pp. 2284-2289, 1999.

[35] B. S. Chen, C. S. Tseng and H. J. Uang, "Mixed H_2/H_∞ fuzzy output feedback control design for nonlinear dynamic systems: An LMI approach," *IEEE Trans. Fuzzy Syst.,* vol. 8, no. 3, pp. 249-265, 2000.

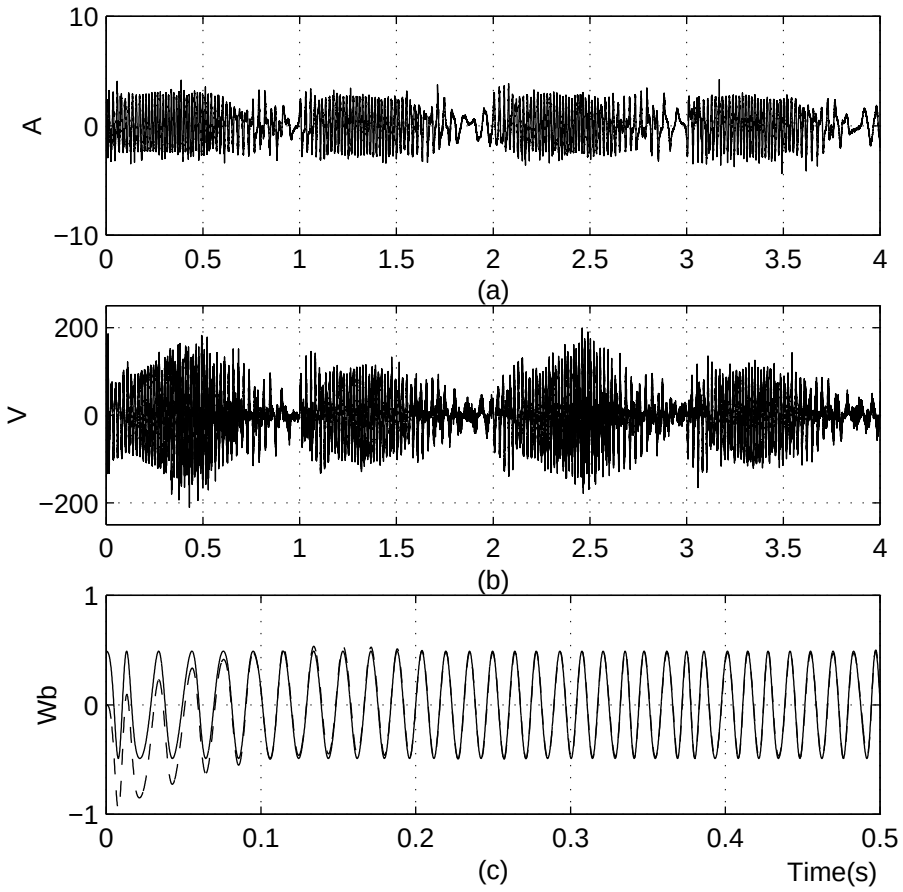

Fig. 10. Sinusoidal speed tracking, (a) primary current for one phase, (b) primary voltage for one phase (c) estimated ($--$) and desired (—) secondary fluxes λ_{sa}.

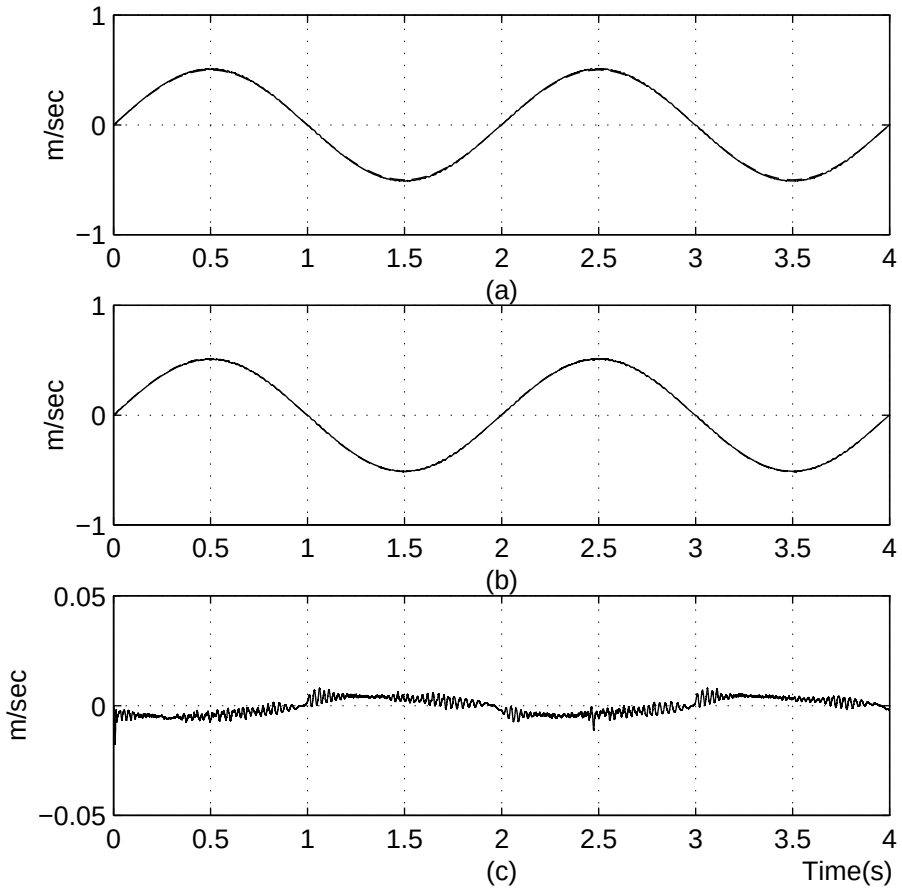

Fig. 11. Sinusoidal speed tracking with parameter uncertainty, (a) desired speed (− −) and actual speed (—), (b) estimated speed (− −) and actual speed (—), (c) speed estimation error.

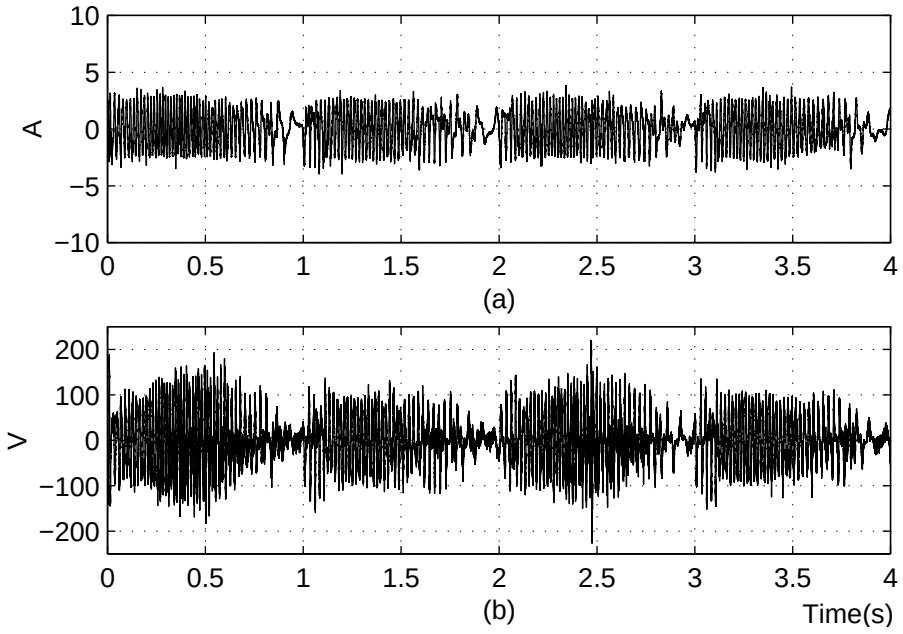

Fig. 12. Sinusoidal speed tracking with parameter uncertainty, (a) primary current for one phase, (b) primary voltage for one phase.

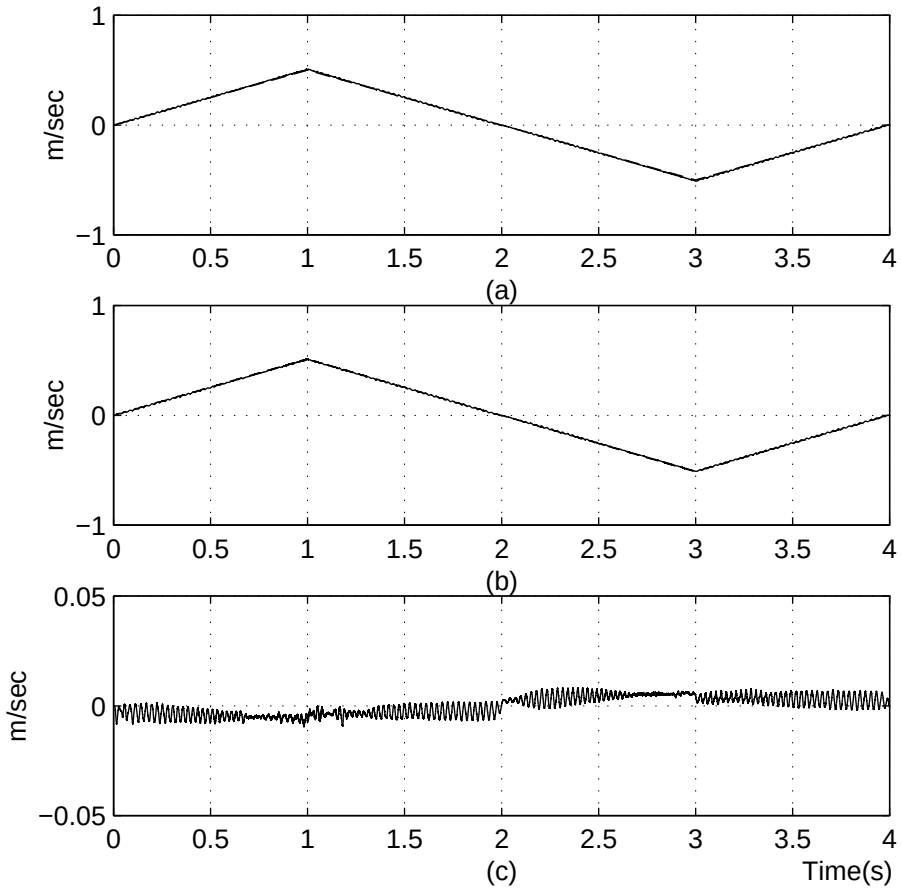

Fig. 13. Triangular speed tracking, (a) desired speed (− −) and actual speed (—), (b) estimated speed (− −) and actual speed (—), (c) speed estimation error.

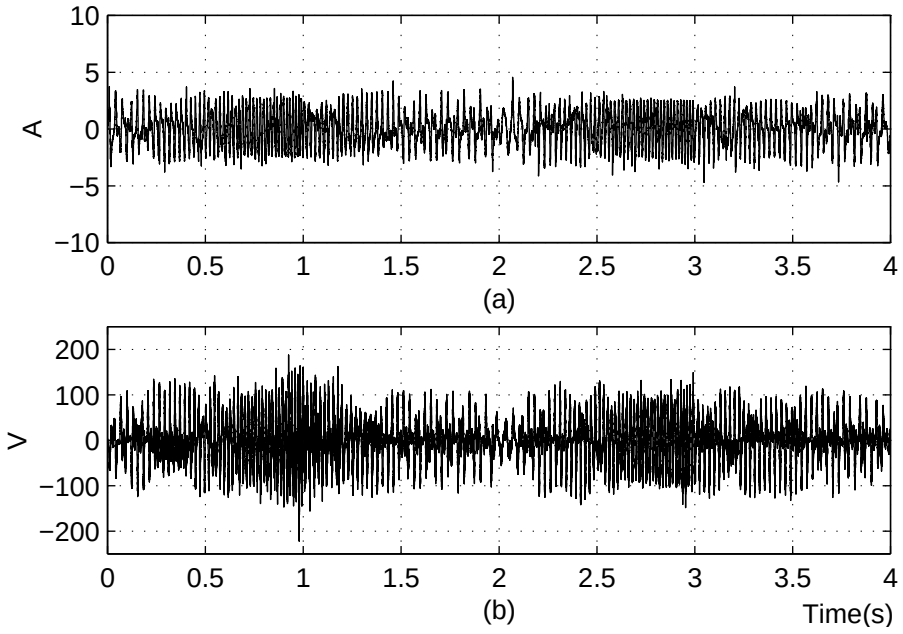

Fig. 14. Triangular speed tracking, (a) primary current for one phase, (b) primary voltage for one phase.

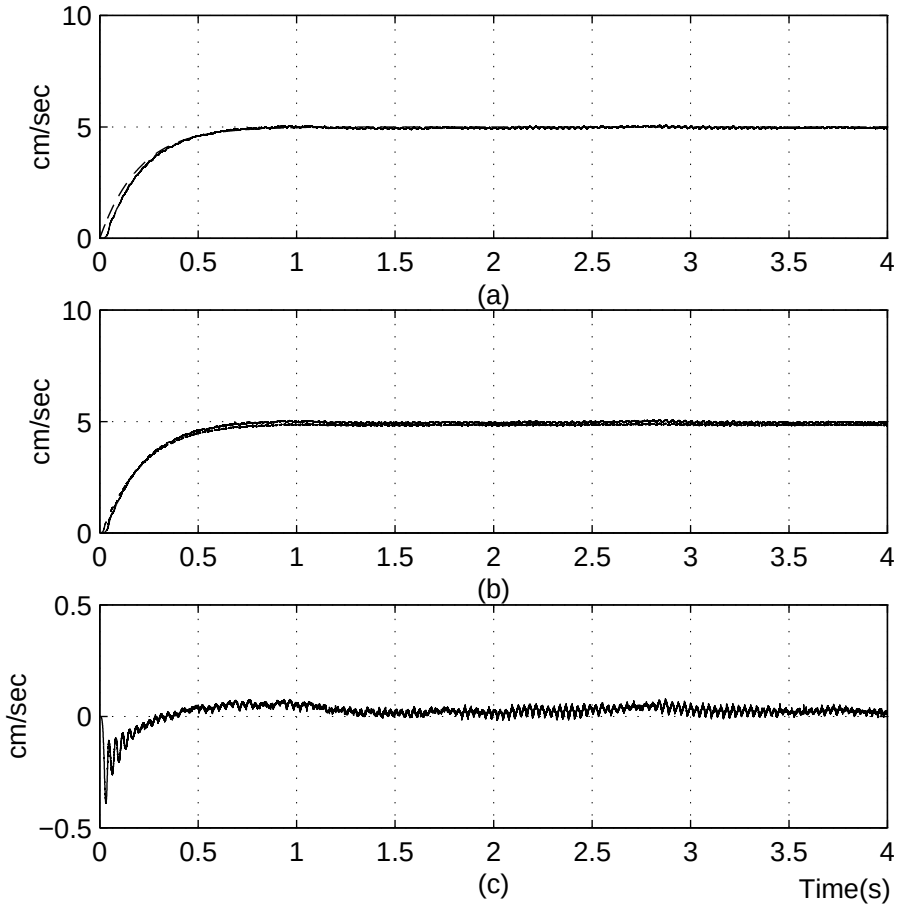

Fig. 15. Low speed regulation, (a) desired speed ($--$) and actual speed (—), (b) estimated speed ($--$) and actual speed (—), (c) speed estimation error.

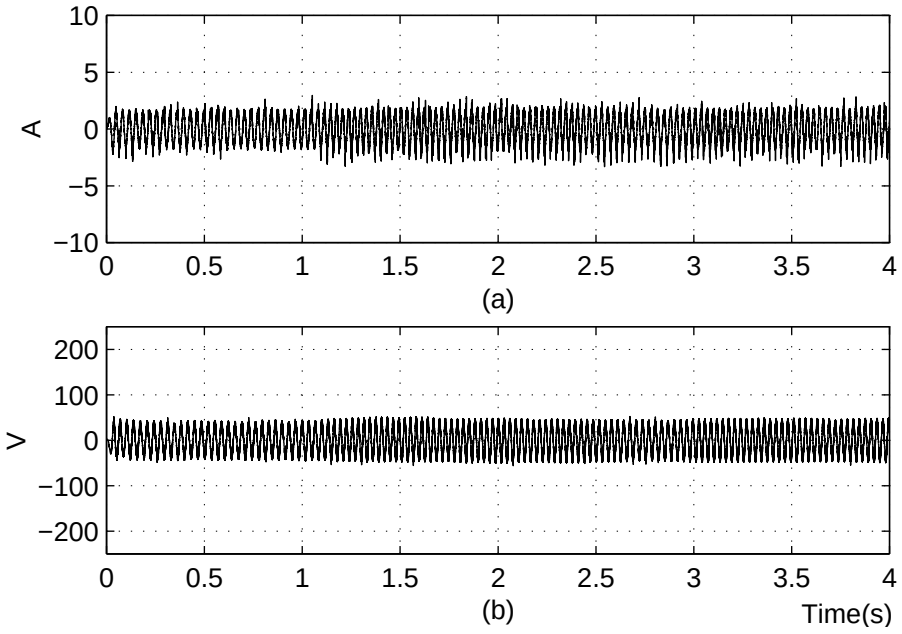

Fig. 16. Low speed regulation, (a) primary current for one phase, (b) primary voltage for one phase.